

# Effect of Pre-deformation on Aging Behavior and Mechanical Properties of Ti-6Al-4V Alloy

Wang Shuliang<sup>1,2,3</sup>, Fu Chaozheng<sup>1,4</sup>, Du Lijing<sup>1</sup>, Li Jingxue<sup>1</sup>, Chen Yuting<sup>1</sup>,  
Liu Li<sup>1</sup>, Fu Chunyan<sup>1</sup>, Huang Yixiong<sup>2</sup>, Xiang Dinghan<sup>3</sup>, Jiang Xiaosong<sup>5</sup>

<sup>1</sup> Southwest Petroleum University, Chengdu 610500, China; <sup>2</sup> Fujian Provincial Key Laboratory of Materials Genome, Xiamen University, Xiamen 361005, China; <sup>3</sup> Guangxi Key Laboratory of Information Materials, Guilin University of Electronic Technology, Guilin 541004, China; <sup>4</sup> Guizhou Aerospace Xinli Forging & Casting Co., Ltd, Zunyi 563003, China; <sup>5</sup> Southwest Jiaotong University, Chengdu 610031, China

**Abstract:** The effects of pre-deformation on the aging behavior and mechanical properties of Ti-6Al-4V alloy were studied. Results show that the pre-deformation after the solution process at 940 and 955 °C is beneficial for promoting the precipitation of the secondary  $\alpha$  phase during the aging of Ti-6Al-4V alloy. When solution temperature is 940 °C, the content of the secondary  $\alpha$  phase increases with the increase of pre-deformation amount, and the size of  $\alpha$  phase decreases. The strength and hardness of the alloy increase monotonously after aging. The tensile strength and hardness of Ti-6Al-4V alloy after aging with pre-deformation are evidently higher than those without pre-deformation. Simultaneously, excellent plasticity is maintained. Compared with solution treatment at 955 °C with pre-deformation, the strength and hardness of Ti-6Al-4V alloy are evidently improved after solution treatment at 940 °C. Scanning electron microscopy examination indicates that the fracture modes of all aged alloys with various pre-deformation degrees are ductile fracture.

**Key words:** Ti-6Al-4V alloy; pre-deformation; aging; mechanical properties

Titanium alloys have been widely used in the aerospace industry, marine resource exploration and development, medical orthopedic implants, and drilling equipment for oil and gas fields because of their high specific strength, excellent corrosion resistance, high and low temperature resistance, and high fatigue strength<sup>[1,2]</sup>. Among these alloys, Ti-6Al-4V (wt%) alloy is first developed and successfully applied; this dual-phase titanium alloy is also the most widely used at present<sup>[3]</sup>. However, given the inadequate strength and hardness of Ti-6Al-4V alloy, it cannot satisfy the performance requirements of some components under certain special circumstances<sup>[4,5]</sup>. At present, Ti-6Al-4V alloy is typically strengthened via the conventional process of solution heat treatment and aging. The tensile strength of Ti-6Al-4V alloy

strengthened via conventional heat treatment can reach approximately 1100 MPa; however, this value cannot satisfy the requirements of some high-strength structural components<sup>[6-8]</sup>. Therefore, a mechanical heat treatment process has been applied by related scientific and technological workers to enhance the strength of Ti-6Al-4V alloy. This process attempts to promote the precipitation of the secondary  $\alpha$  phase during aging by defects, such as dislocations, generated during deformation<sup>[9,10]</sup>. However, the deformation stage of mechanical heat treatment is performed at extremely high temperatures; hence, dynamic recovery and recrystallization will occur during deformation, which reduce or even eliminate dislocations and other crystal defects. Thus, the defects that remain at room temperature after cooling slightly affect the

Received date: July 20, 2019

Foundation item: Open Fund of Guangxi Key Laboratory of Information Materials, Guilin University of Electronic Technology (191009-K); Scientific Research Foundation and Opening Foundation of Southwest Petroleum University (X151518KCL23); Open Fund of Fujian Provincial Key Laboratory of Materials Genome, Xiamen University

Corresponding author: Wang Shuliang, Ph. D., Associate Professor, School of Materials Science and Engineering, Southwest Petroleum University, Chengdu 610500, P. R. China, Tel: 0086-028-83037417, E-mail: wsliang1465@126.com

Copyright © 2020, Northwest Institute for Nonferrous Metal Research. Published by Science Press. All rights reserved.

precipitation of the second phase in the subsequent aging process, and the mechanical properties of the alloy cannot be improved considerably. In addition to heat treatment strengthening, the strength of Ti-6Al-4V alloy can be improved by severe plastic deformation and alloying. However, the plasticity of the alloy is simultaneously reduced to various degrees, resulting in the poor toughness of the alloy, which cannot satisfy the performance requirements of high strength and toughness for the structural components of titanium alloy<sup>[11-16]</sup>.

Several researches have reported that the solution method and subsequent pre-deformation and aging (deformation and aging synergism) can be adopted to strengthen metal materials. In the study of metastable  $\beta$ -titanium alloy, pre-deformation can promote the precipitation of  $\alpha$  phase and make it selective in its growth direction. The strengthening efficiency of the deformation and aging synergism is better than that of the conventional heat treatment. At the same strength level, the toughness of the alloy strengthened by the former is higher than that strengthened by the latter, and the peak aging time of the former is shorter than that of the latter<sup>[17,18]</sup>. Thus, the solution process with subsequent pre-deformation and aging is a promising technique for improving the strength of titanium alloys. For the widely used Ti-6Al-4V alloy, the effects of pre-deformation and aging synergism on microstructure evolution and mechanical properties have seldom been reported. Therefore, the effects of pre-deformation after the solution process on the aging precipitation behavior and mechanical properties of Ti-6Al-4V alloy were investigated. The results are highly significant in improving the safety of Ti-6Al-4V alloy and broadening its application field.

## 1 Experiment

A typical dual-phase titanium alloy, namely, Ti-6Al-4V, was selected. The chemical composition of the as-received Ti-6Al-4V alloy is provided in Table 1. After solution treatment at 940 and 955 °C for 30 min and cooled in water, Ti-6Al-4V alloy rods were made into tensile samples with a gauge length of 32 mm and a diameter of 7 mm. The tensile samples solution-treated at 940 °C were drawn to 0.00, 0.03, 0.05,

0.05, and 0.07 engineering strain, whereas the tensile samples solution-treated at 955 °C were drawn to 0 and 0.07 engineering strain at a rate of 2 mm/min at room temperature, as shown in Fig.1. All the pre-deformed and un-pre-deformed specimens were aged at 500 °C for 4 h and cooled in air. The final tensile samples were made by processing the pre-deformed and aged test pieces into 12 mm gauge length and 5 mm diameter, as shown in Fig.2. Tensile tests were conducted on a WDW-1000 computer-controlled electronic universal experiment machine at a rate of 1 mm/min.

Specimens for metallographic, X-ray diffraction (XRD) analysis, and microhardness examinations were cut from the pre-deformed section. Metallographic samples were prepared and etched in a reagent containing 5 vol% HF+10 vol% HNO<sub>3</sub>+85 vol% H<sub>2</sub>O. A DME-300M optical microscope was used to observe microstructural characterization. Vickers hardness experiments were performed on an HXD-2000TM/LCD microhardness instrument with a load of 5 N and a holding time of 10 s. Phase analyses were implemented on a DX-2700 X-ray diffractometer using a Cu K $\alpha$  radiation source with an accelerating voltage of 40 kV and a current of 30 mA. Tensile fracture surfaces were observed using a ZEISS EV0 MA15 scanning electron microscope with an accelerating voltage of 20 kV. The static toughness values of the aged alloys were determined using Origin software to calculate the area surrounded by their tensile stress-strain curve.

## 2 Results and Discussion

### 2.1 Phase analysis via XRD

Fig.3a shows the XRD patterns of the samples after solution treatment at 940 and 955 °C for 30 min and water quenching. As shown in the diagram, the samples after solution treatment at the two aforementioned temperatures are composed of the  $\alpha$ ,  $\beta$ , and  $\alpha'$  (martensite) phases. The XRD patterns of these samples aged at 500 °C for 4 h after

**Table 1 Chemical composition of the as-received Ti-6Al-4V alloy (wt%)**

Al	V	Fe	C	N	O	H	Ti
6.2	4.1	≤0.3	≤0.08	≤0.05	≤0.2	≤0.015	Bal.

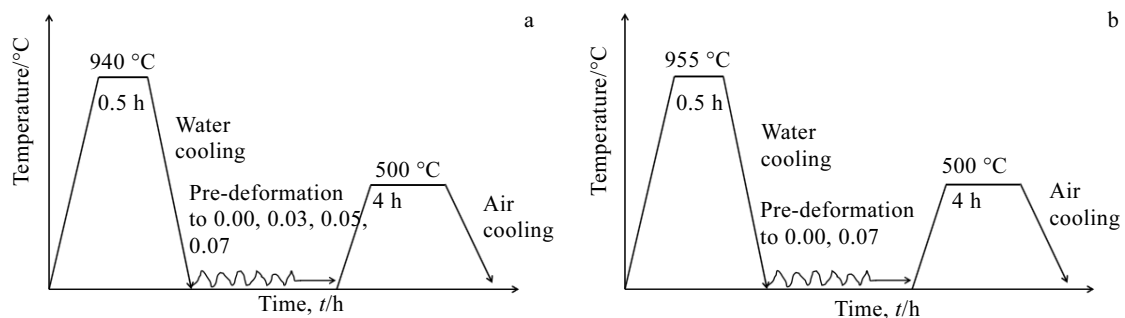


Fig.1 Schematic of the heat treatment process

solution treatment at 940 and 955 °C with various pre-deformations are summarized in Fig.3b and 3c, respectively. The XRD patterns show that the microstructure under different heat treatment conditions consists only of  $\alpha$  and  $\beta$  phases.

## 2.2 Effect of pre-deformation on microstructure of Ti-6Al-4V Alloy

Fig.4 compares the optical microstructures of the Ti-6Al-4V samples that were solution treated at 940 °C and aged at 500 °C for 4 h with various pre-deformations. The figure shows the following characteristics. (1) The microstructure of all the samples consists of the equiaxed primary  $\alpha$  phase, lamellar secondary  $\alpha$  phase and  $\beta$  phase. (2) The diameter of the primary  $\alpha$  phase in the pre-deformed samples is evidently reduced compared with the sample that was aged directly after solution treatment (without pre-deformation). (3) The amount of the lamellar secondary  $\alpha$  phase considerably increases as the pre-deformation strain increases from 0.00 to 0.07, and its size decreases gradually. Thus, the pre-deformation for Ti-6Al-4V alloy after solution treatment can promote the precipitation of the secondary  $\alpha$  phase during the aging process.

Fig.5a and 5b illustrate the optical microstructures of Ti-6Al-4V specimens that were aged at 500 °C for 4 h with 0.00 and 0.07 pre-deformation, respectively after solution treatment at 955 °C. The microstructures with 0.00 and 0.07 pre-deformations consist of a spot of the equiaxed primary  $\alpha$  phase, lamellar secondary  $\alpha$  phase and  $\beta$  phase. Compared with the optical microstructure of the sample without pre-deformation, the size of the secondary  $\alpha$  phase in the pre-deformed samples is gradually reduced. Evidently, after solution treatment at 955 °C, the promoting efficiency of pre-deformation on the precipitation of the secondary  $\alpha$  phase is weaker than that at 940 °C.

In the pre-deformation process, dislocations, distortion energy, and vacancy-type defects are produced in the solution-treated alloys. When the solution-treated and pre-deformed Ti-6Al-4V alloys were subjected to aging, the lamellar secondary  $\alpha$  phases may nucleate in the regions

with high dislocation density to reduce the energy barrier of nucleation<sup>[19]</sup>. Therefore, the defect produced during pre-deformation provides more nucleation positions for the precipitation of the secondary  $\alpha$  phase during the subsequent aging process, i.e., the pre-deformed sample exhibits a high nucleation rate. The secondary  $\alpha$  phase easily nucleates in the defect position, and the  $\alpha$  phase gradually occupies the dislocation position, thereby decreasing the dislocation density of these components, and the strain energy stored in the original dislocation is gradually released when the dislocations disappear. The released energy reduces the energy barrier of the nucleation and growth of the secondary  $\alpha$  phase, which is beneficial for the decomposition of the supersaturated solid solution and is a driving force of phase transition<sup>[17]</sup>. The decomposition of metastable phases ( $\alpha'$  martensite or metastable  $\beta$ ) in titanium alloy belongs to diffusive transformation. The diffusion-type phase transformation requires channels, and defects, such as vacancies and dislocations, produced during pre-deformation provide channels for the diffusion of atoms, which are conducive to the precipitation of the secondary  $\alpha$  phase during the aging process<sup>[20]</sup>.

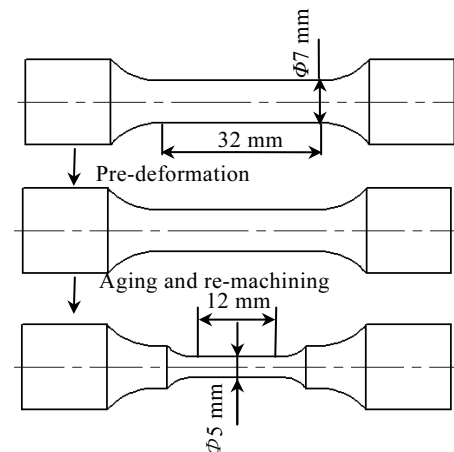


Fig.2 Schematic of heat treatment and machining procedures of the tensile specimens

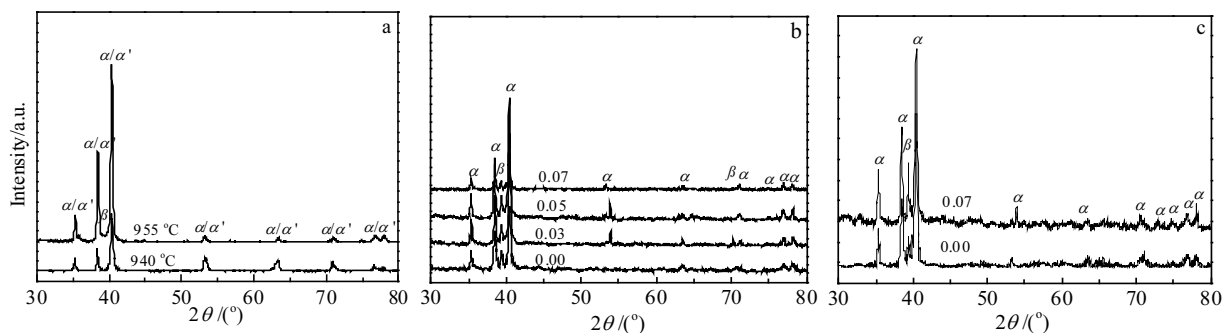


Fig.3 XRD patterns of Ti-6Al-4V: (a) solution treatment at 940 and 955 °C for 30 min and water cooling, (b) solution treatment at 940 °C for 30 min and aging at 500 °C for 4 h with various pre-deformations, and (c) solution treatment at 955 °C for 30 min and aging at 500 °C for 4 h with various pre-deformations

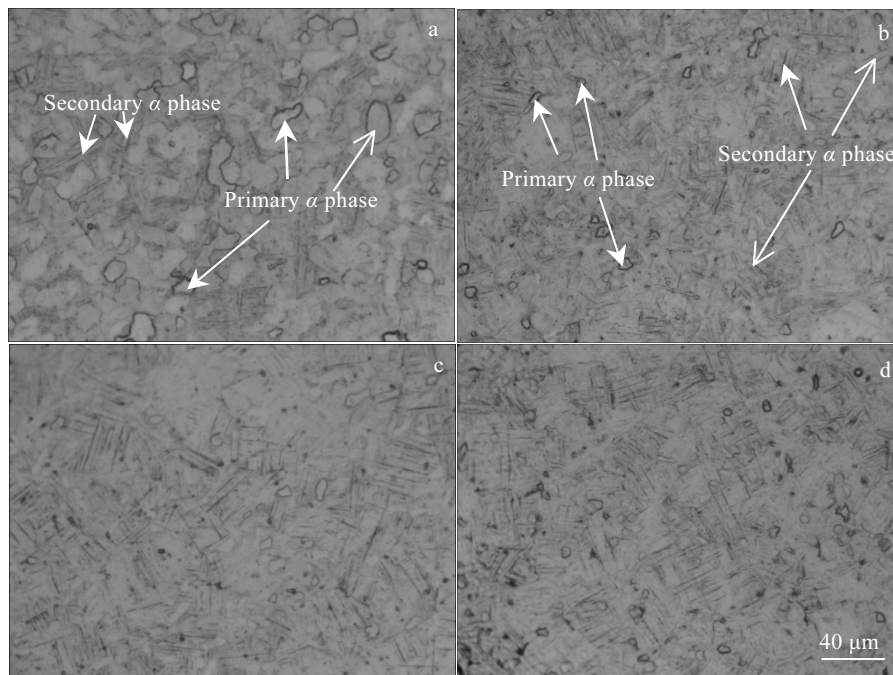


Fig.4 Optical micrographs of Ti-6Al-4V samples aged at 500 °C for 4 h after solution treatment at 940 °C with different pre-deformations: (a) 0.00, (b) 0.03, (c) 0.05, and (d) 0.07

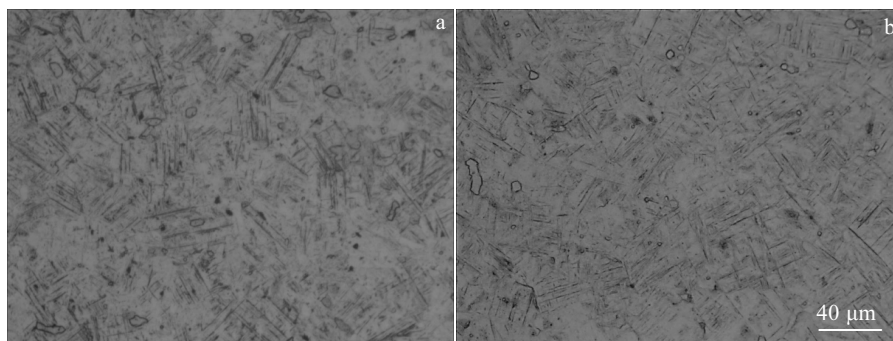


Fig.5 Optical micrographs of Ti-6Al-4V samples aged at 500 °C for 4 h after solution treatment at 955 °C without (a) and with 0.07 pre-deformation (b)

The existence of dislocations reduces the diffusion barrier of solute atoms and facilitates the diffusion of atoms. Thus, the kinetic process of phase transition in the secondary  $\alpha$  phase is accelerated<sup>[17]</sup>. Therefore, more defects appear in the crystal of the solution-treated alloy when pre-deformation is large, and the secondary  $\alpha$  phase after aging is small under the same conditions. The microstructures of the lamellar martensite obtained after solution treatment at 955 °C are larger than that after solution treatment at 940 °C, which results in poor plasticity. During subsequent pre-deformations, deformation is conducted by the equiaxed primary  $\alpha$  phase, and fewer dislocations and other defects are observed in martensite. Thus, when the solution temperature is 955 °C, the promoting efficiency of

pre-deformation on the precipitation of the secondary  $\alpha$  phase is weaker than that at 940 °C. The metastable phase obtained from the solution-treated Ti-6Al-4V alloy is mostly the  $\alpha'$  phase, and the metastable  $\beta$  phase is rare. Using the decomposition process of the  $\alpha'$  phase as an example, the schematic of the nucleation and growth of the secondary  $\alpha$  phases of Ti-6Al-4V alloy without and with pre-deformation is shown in Fig.6.

### 2.3 Effect of pre-deformation on mechanical properties of Ti-6Al-4V Alloy

Fig.7a and 7b show the effect of pre-deformation after solution treatment at 940 °C on the mechanical properties of Ti-6Al-4V alloy. The results indicate that the yield strength ( $\sigma_{0.2}$ ), ultimate tensile strength ( $\sigma_b$ ), and hardness

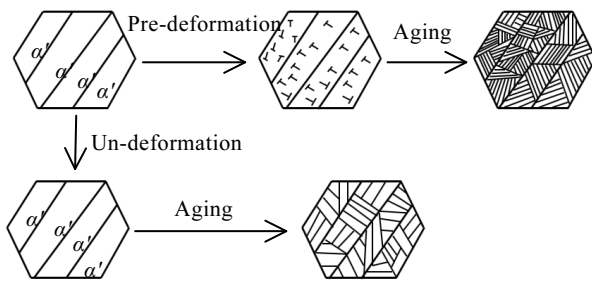


Fig.6 Schematic of nucleation and growth of secondary  $\alpha$  phase in Ti-6Al-4V alloy without and with pre-deformation

gradually increase with the increase of pre-deformation value; simultaneously, excellent plasticity is maintained. Strength considerably increases when pre-deformation increases from 0.00 to 0.03. The increments of  $\sigma_{0.2}$  and  $\sigma_b$  are approximately 11.73% and 8.93%, respectively. Strength increases slowly under the same aging treatments as pre-deformation continues to increase from 0.03 to 0.07. When pre-deformation increases to 0.07, the maximum values of strength and hardness are obtained. The  $\sigma_{0.2}$  and  $\sigma_b$  of the pre-deformed samples increase by approximately 136 and 114 MPa, respectively, compared with that of the un-pre-deformed samples with the same aging treatments.

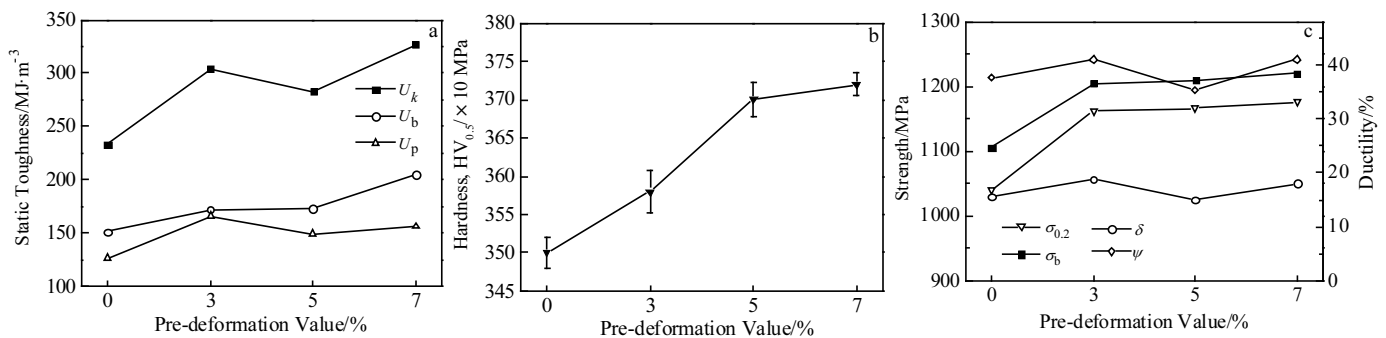


Fig.7 Static toughness (a), microhardness (b), and strength and plasticity (c) versus pre-deformation of Ti-6Al-4V alloy after solution treatment at 940 °C for 30 min ( $U_k$  denotes total static toughness,  $U_b$  denotes static toughness before necking, and  $U_p$  denotes the static toughness of the plastic deformation stage)

Evidently, the strength of the pre-deformed samples is larger than that of the samples without pre-deformation. The tensile strength of the pre-deformed alloy can reach more than 1200 MPa, which is close to the level of ultrahigh strength ( $\sigma_b \geq 1250$  MPa). This result cannot be achieved via conventional heat treatment including solution and aging. Fig.7c presents the relationship between pre-deformation and static toughness. As shown in the figure, all the static toughness values of Ti-6Al-4V alloy with pre-deformation increase due to the increase in strength, and plasticity remains excellent.

Fig.8a and 8b illustrate the effects of pre-deformation after solution treatment at 955 °C on the strength, microhardness, and ductility of Ti-6Al-4V alloy. The two diagrams show that the tensile strength and microhardness of the pre-deformed and aged samples are higher than those of the aged sample without pre-deformation. When pre-deformation is conducted, the yield strength  $\sigma_{0.2}$  and ultimate tensile strength  $\sigma_b$  increase by approximately 25 and 18 MPa, respectively, but the increment in strength is considerably lower than that of the sample that is solution-treated at 940 °C (Fig. 7a). No evident change in the elongation  $\delta$  and reduction of the area  $\psi$  of the pre-deformed samples are observed compared with the

un-pre-deformed samples with the same aging treatments. As presented in Fig.8c, the static toughness values of Ti-6Al-4V alloy increase with pre-deformation.

As shown in Fig.4 and Fig.5, dislocations and distortion energy are produced in the solution-treated alloy during pre-deformation, which increase the nucleation rate of the secondary  $\alpha$  phase during aging. When the supersaturated solid solution has numerous defects, the secondary  $\alpha$  phase after aging is small under the same conditions. Moreover, when the content of the secondary  $\alpha$  phase is high, the precipitation enhancement triggered by secondary  $\alpha$  phase is strong; thus, the strength of Ti-6Al-4V alloy increases with pre-deformation. In addition, given that the diameter of the primary  $\alpha$  phases in the pre-deformed samples is smaller than that in the un-pre-deformed samples, the effect of fine grain strengthening can be increased, which also increases the strength of the pre-deformed samples<sup>[15, 21]</sup>.

As shown in Fig.5, when solution temperature is 955 °C, the promoting efficiency of pre-deformation on the precipitation of the secondary  $\alpha$  phase is weak; thus, the microstructure of the aged sample with 0.07 pre-deformation is slightly different from that of the sample without pre-deformation. In addition, the increments in strength are relatively small, and the elongation  $\delta$  and reduction of the

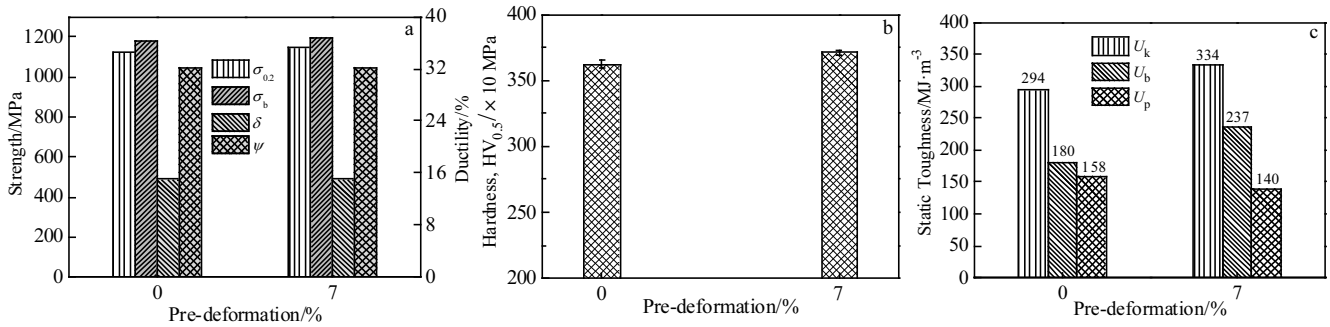


Fig.8 Strength and ductility (a), microhardness (b), and static toughness (c) of Ti-6Al-4V alloy after solution treatment at 955 °C for 30 min

area  $\psi$  present no evident change. When pre-deformation increases from 0.00 to 0.07, the elongation and reduction of the area remain under excellent condition in the Ti-6Al-4V samples solution treated at 940 and 955 °C with the same aging treatments (Fig.7a and 8a), even if strength markedly increases (Fig.7a). This finding may be attributed to the fine microstructure of the pre-deformed samples. Thus, more grains bear deformation, and stress does not concentrate locally, which causes cracks to appear prematurely. Moreover, dislocation density in the solution-treated and pre-deformed samples decreases with the precipitation of the  $\alpha$  phase during aging. This condition is another reason for the excellent plasticity of the pre-deformed and aged samples. Song et al.<sup>[17]</sup> reported that the excellent plasticity of the aged samples with pre-deformation may be related to the formation of massive fractions of parallel  $\alpha$  platelets. As schematically shown in Fig.9, a dislocation cannot easily slip into the matrix with interlaced  $\alpha$  platelets (Fig.9a), but it can easily slip into the matrix with parallel  $\alpha$  platelets (Fig.9b). Therefore, the formation of parallel  $\alpha$  platelets during aging may be beneficial for improving the ductility and static toughness of Ti-6Al-4V alloy. In the current

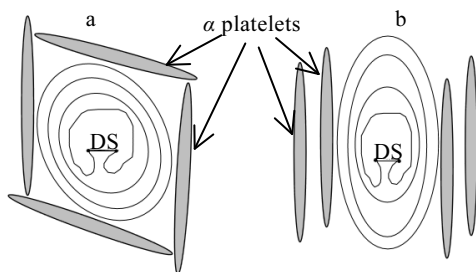


Fig.9 Schematic diagram of the effect of the variant selection of  $\alpha$  platelets on dislocation evolution: (a) without effect and (b) with variant selection effect (DS denotes dislocation source)<sup>[17]</sup>

study, a large number of parallel  $\alpha$  platelets are not observed in the aged samples with pre-deformation compared with the microstructure of the aged samples without pre-deformation. Therefore, the contribution of parallel  $\alpha$  platelets to plasticity improvement may be insignificant.

## 2.4 Fracture morphology

Fracture surfaces were observed via scanning electron microscopy (SEM) to gain an insight into the influence of pre-deformation on fracture behavior after stretching in Ti-6Al-4V alloy. Fig.10 shows the macroscopic fracture morphology of Ti-6Al-4V samples after solution treatment at 940 °C and aging at 500 °C for 4 h with various pre-deformations. At room temperature, the tensile fracture surfaces of all the specimens are cup-cone shaped. The fracture surfaces are composed of the fiber region at the center and the shear lip region at the edge (Fig.10b), but the radiation zone cannot be observed clearly. The fiber region is separated from the shear lip by a distinct boundary. This region is dark gray without metallic gloss, and does not exhibit a granular appearance. These characteristics indicate a ductile fracture. The shear lips of all the specimens are smooth at 45° in the direction of the tensile axis and account for a small proportion of the total fracture area (Fig.10b). These characteristics indicate a typical severed fracture.

Fig.11 illustrates the microscopic fracture morphology of the fiber region of the Ti-6Al-4V samples after solution treatment at 940 °C and aging at 500 °C for 4 h with various pre-deformations. The figure clearly shows that the fiber region of all the samples consists of a large number of dimples, indicating that the fracture modes of all the samples are primarily ductile fracture. The dimples of the samples with 0.05 pre-deformation are shallower and denser than those of other samples, indicating that the ductility of this sample is poor. This result is consistent with that shown in Fig.7a and may be attributed to the large length-to-width ratio of the lamellar  $\alpha$  phase, which results in the poor plasticity of the sample. The fractographs show that many holes

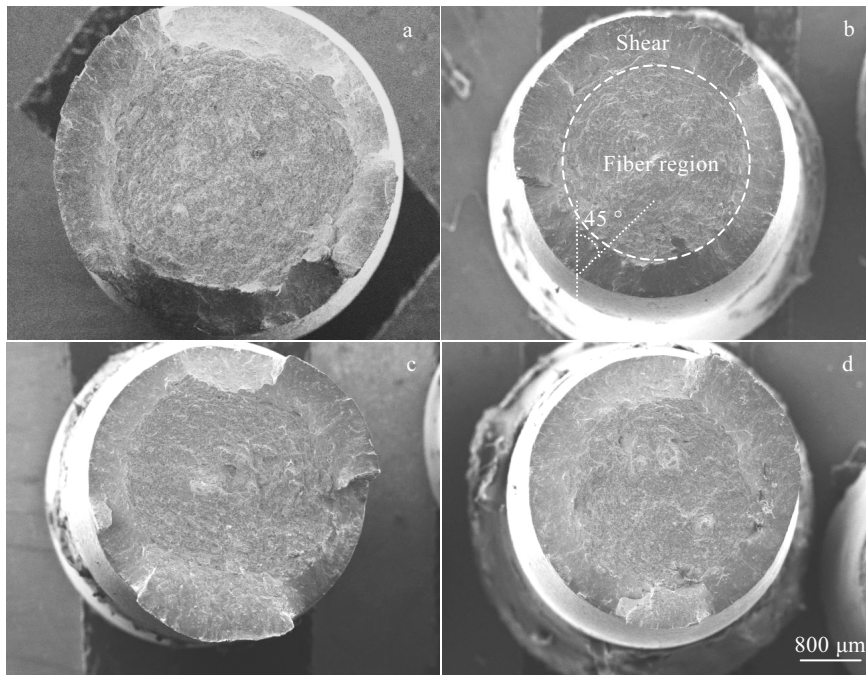


Fig.10 SEM images of fracture surfaces of Ti-6Al-4V samples solution treated at 940 °C and aged at 500 °C for 4 h with different pre-deformations: (a) 0.00, (b) 0.03, (c) 0.05, and (d) 0.07

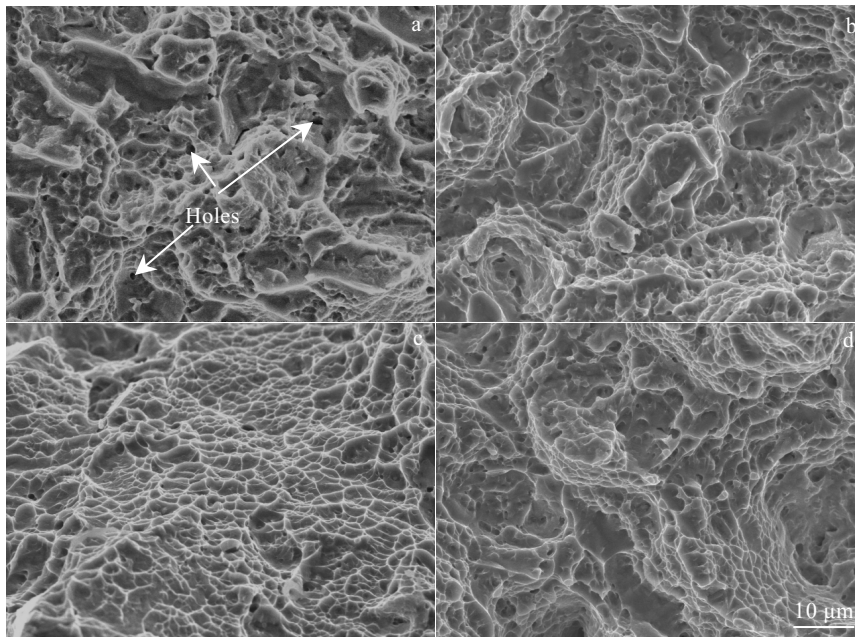


Fig.11 SEM images of fracture surfaces of fiber region of Ti-6Al-4V samples solution treated at 940 °C and aged at 500 °C for 4 h with different pre-deformations: (a) 0.00, (b) 0.03, (c) 0.05, and (d) 0.07

exist in the fiber region of all the samples due to the dislocation accumulation at the interface between the  $\alpha$  phase and the  $\beta$  matrix, thereby leading to stress concentration and the nucleation and formation of holes at the  $\alpha/\beta$  phase interface<sup>[22]</sup>.

Fig.12a and 12b show the macroscopic fracture morphologies of the Ti-6Al-4V samples after solution treatment

at 955 °C and aging at 500 °C for 4 h with 0.00 and 0.07 pre-deformation, respectively. Similar to the tensile fracture surfaces of the specimens with a solution temperature of 940 °C, the tensile fracture surfaces of the two specimens after solution treatment at 955 °C exhibit a cup-cone shape after stretching at room temperature. The fracture surfaces are also composed of the fiber region at the center and the

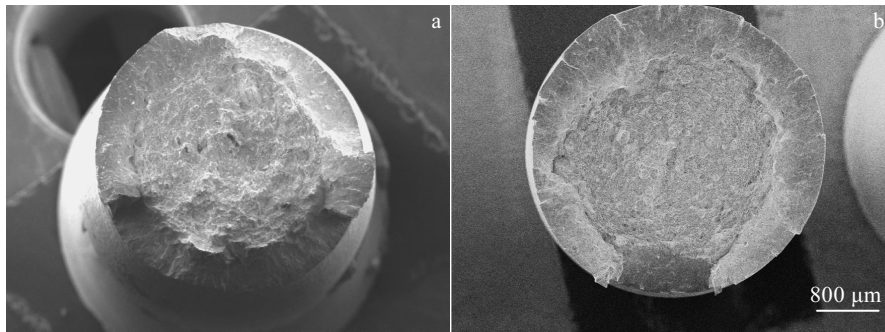


Fig.12 SEM images of fracture surfaces of Ti-6Al-4V samples solution treated at 955 °C and aged at 500 °C without (a) and with 0.07 pre-deformation (b)

shear lip region at the edge. The fiber region is separated from the shear lip by a distinct boundary, thereby indicating ductile fracture characteristic.

Fig.13 illustrates the microscopic fracture morphology of the fiber region of Ti-6Al-4V samples after solution treatment at 955 °C and aging at 500 °C for 4 h with different pre-deformations. Evidently, dimples prevail in the entire fracture surface of the two specimens without and with pre-deformation, which indicates that the fracture modes of

these samples are trans-granular ductile fracture. No significant difference is observed in the depth and size of the dimples in the fiber zone because the microstructures of the two samples are similar (Fig.13). The fractographs also show that numerous micro-holes exist in the fiber region of the two samples probably due to the dislocation accumulation at the interface between the  $\alpha$  phase and  $\beta$  matrix, which leads to stress concentration and the nucleation and formation of micro-holes at the  $\alpha/\beta$  phase interface<sup>[22]</sup>.

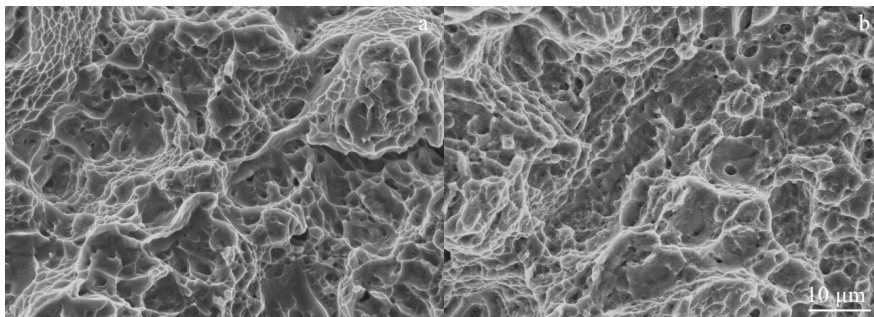


Fig.13 SEM images of fracture surfaces of fiber region of Ti-6Al-4V samples solution treated at 955 °C and aged at 500 °C without (a) and with 0.07 pre-deformation (b)

### 3 Conclusions

1) The size of the primary  $\alpha$  phase decreases when pre-deformation is conducted on Ti-6Al-4V alloy after solution treatment, and the pre-deformation is beneficial for promoting the precipitation of the secondary  $\alpha$  phase during the aging process. The increase in pre-deformation amount increases the content of the secondary  $\alpha$  phase but decreases its size.

2) The strength, hardness, and static toughness of Ti-6Al-4V alloy increase after aging with pre-deformation, and the tensile strength and hardness of Ti-6Al-4V alloy with pre-deformation are evidently higher than those of Ti-6Al-4V alloy without pre-deformation. Simultaneously, excellent plasticity is maintained, and the fracture modes of

all the samples with different pre-deformations are ductile fracture.

3) When the solution temperature is 940 °C, the promoting efficiency of pre-deformation on the precipitation of the secondary  $\alpha$  phase is higher than that at 955 °C, and the increment in the strength, hardness, and static toughness of Ti-6Al-4V alloy is considerably higher than that of the sample solution-treated at 955 °C.

### References

- 1 Sharif S, Rahim E A. *Journal of Materials Processing Technology*[J], 2007, 185: 72
- 2 Fojt J, Filip V, Joska L. *Applied Surface Science*[J], 2015, 355: 52
- 3 Obasi G C, Biroasca S, Prakash D G L et al. *Acta Materi-*

- alia[J], 2012, 60(17): 6013
- 4 Bantounas I, Lindley T C, Rugg D et al. *Acta Materialia*[J], 2007, 55(16): 5655
  - 5 Vajpai S K, Ota M, Watanabe T et al. *Metallurgical and Materials Transactions A*[J], 2015, 46(2): 903
  - 6 Liu W Y, Lin Y H, Chen Y H et al. *Rare Metal Materials and Engineering*[J], 2017, 46(3): 634
  - 7 Filip R, Kubiak K, Ziaja W et al. *Journal of Materials Processing Technology*[J], 2003, 133(1): 84
  - 8 Abbasi S M, Momeni A. *Transactions of Nonferrous Metals Society of China*[J], 2011, 21(8): 1728
  - 9 Peng X N, Guo H Z, Shi Z F et al. *Transactions of Nonferrous Metals Society of China*[J], 2014, 24(3): 682
  - 10 Sun L P, Lin G Y, Liu J et al. *Journal of Central South University of Technology*[J], 2010, 17(3): 443
  - 11 Semenova I P, Raab G I, Saitova L R et al. *Materials Science and Engineering A*[J], 2004, 387: 805
  - 12 Sergueeva A V, Stolyarov V V, Valiev R Z et al. *Scripta Materialia*[J], 2000, 43(9): 819
  - 13 Wang Y C, Langdon T G. *Materials Science and Engineering A*[J], 2013, 559(3): 861
  - 14 Choe H, Abkowitz S M, Abkowitz S et al. *Materials Science and Engineering A*[J], 2005, 396(1-2): 99
  - 15 Singh G, Sen I, Gopinath K et al. *Materials Science and Engineering A*[J], 2012, 540(1): 142
  - 16 Kanou O, Fukada N, Hayakawa M. *Materials Transactions*[J], 2016, 57(5): 681
  - 17 Song Z Y, Sun Q Y, Xiao L et al. *Materials Science and Engineering A*[J], 2010, 527(3): 691
  - 18 Guo Q, Wang Q, Han X L et al. *Rare Metal Materials and Engineering*[J], 2011, 40(3): 377
  - 19 Furuhashi T. *Metals and Materials*[J], 2000, 6(3): 221
  - 20 Wan M P, Zhao Y Q, Zeng W D et al. *Journal of Alloys and Compounds*[J], 2015, 619: 383
  - 21 Lu K, Lu L, Suresh S. *Science*[J], 2009, 324(17): 349
  - 22 Castany P, Sturmel F P, Douin J et al. *Materials Science and Engineering A*[J], 2008, 483(1): 719

## 预变形对 Ti-6Al-4V 合金时效行为和力学性能的影响

王书亮<sup>1,2,3</sup>, 付朝政<sup>1,4</sup>, 杜丽婧<sup>1</sup>, 李婧雪<sup>1</sup>, 陈雨婷<sup>1</sup>, 刘 丽<sup>1</sup>, 付春艳<sup>1</sup>, 黄艺雄<sup>2</sup>, 向定汉<sup>3</sup>, 蒋小松<sup>5</sup>

(1. 西南石油大学, 四川 成都 610500)

(2. 厦门大学 福建省材料基因重点实验室, 福建 厦门 361005)

(3. 桂林电子科技大学 广西省信息材料重点实验室, 广西 桂林 541004)

(4. 贵州航天新力铸锻有限责任公司, 贵州 遵义 563003)

(5. 西南交通大学, 四川 成都 610031)

**摘要:** 研究了固溶处理后预变形对 Ti-6Al-4V 合金时效行为和力学性能的影响。结果表明: 在 940 和 955 °C 固溶处理后进行预变形, 可以提高时效过程中第二相  $\alpha$  的析出。在 940 °C 固溶处理后, 随着预变形量的增加, 时效处理后第二相  $\alpha$  含量增加,  $\alpha$  相尺寸减小, 合金的强度和硬度增加。在时效处理之前进行预变形可以明显提高合金的抗拉伸强度和硬度, 也能同时保持比较好的韧性。相对固溶温度为 940 °C, Ti-6Al-4V 合金在 955 °C 固溶处理后进行预变形对于提高合金的强度和硬度的效果不显著。采用扫描电镜对不同预变形和时效处理后的合金断口形貌进行了分析。

**关键词:** Ti-6Al-4V 合金; 预变形; 时效; 力学性能

作者简介: 王书亮, 男, 1978 年生, 博士, 副教授, 西南石油大学材料科学与工程学院, 四川 成都 610500, 电话: 028-83037417, E-mail: wsliang1465@126.com